P1.19 Retrieval of Cloud Liquid Water Content Profiles with Radar and Lidar: Application to Multi-annual Data Sets and Comparison with Microphysical Cloud Simulation.

Oleg Krasnov, Herman Russchenberg, Delft University of Technology, Delft, Netherlands;
Alexander Khain, and Mark Pinsky, Hebrew University of Jerusalem, Israel

1. INTRODUCTION

The parameterization of the microphysical characteristics for low-level stratiform water clouds can be developed in terms, among others, of the *effective radius of droplets* and the *liquid water content* (*LWC*). These parameters can be directly measured using aircraft mounted in-situ probes observations. The instruments used to perform these measurements, however, have an extremely small sample volume. The remote sensing methods are less direct but give much better coverage and are less expensive.

As it was noted in many studies (e.g. Fox and Illingworth (1997)), there are some problems in applicability of the radar measurements alone for the retrieval of the mentioned above parameters. Small number of big particles (so-called drizzle) can produce the major part of the cloud's reflectivity *Z* without strong contribution in the LWC and effective radius. A few *Z-LWC* relations were published in literature, but all of them are noted as applicable only in absence of drizzle. From other point of view, in many studies were noted that the presence of the drizzle fraction in water clouds is more usual than its absence (e.g. Gerber (1996), Fox and Illingworth (1997)). All these facts give the motivation for the efforts to find the combination of the remotely measurable parameters, which can be used for the detection of drizzle fraction, its parameterization and taking into account in cloud's microphysics retrieval algorithm.

In this paper a retrieval technique based on the possibilities to characterize drizzle fraction in water clouds using the ratio between simultaneously measured radar reflectivity and lidar's optical extinction profiles is presented. This parameter is using for the detection of the presence of drizzle particles in water clouds and the classification of water cloud cells into three classes – "the cloud without drizzle", "the cloud with light drizzle" and "the cloud with heavy drizzle". Different relationships between the radar reflectivity and liquid water content then can be applied for different types of cloud cells to retrieve actual liquid water content.

The paper is organized as follow. Section 2 describes the study of in-situ measured spectra of water drops in low level clouds. It includes the description of used datasets from a few experimental campaigns, gives the statistically based definition of drizzle in water clouds, characterizes the drizzle influence on remote sensing measurables and LWC, shows the possibility to use radar reflectivity to lidar optical extinction ratio for drizzle detection and clouds categorization into three classes - "the cloud without drizzle", "the cloud with light drizzle" and "the cloud with heavy drizzle". Different relationships between the radar reflectivity and liquid water content then can be applied for different types of cloud cells to retrieve actual liquid water content. Section 3 addresses the possible implementation of retrieved relationships as background for the remote sensing retrieval technique. Sections 4 and 5 presents the details and results of the proposed technique applied to the multiyear radar and lidar data from the Cloudnet dataset, including validation using LWP from microwave radiometers. In section 6 briefly formulated conclusions are given.

2. THE ANALYSIS OF THE IN-SITU DROPSIZE DISTRIBUTIONS

2.1. Observational data used

The CLARE'98 campaign. The Cloud Lidar and Radar Experiment (CLARE) took place near Chilbolton (United Kingdom) in October 1998. This extensive cloud campaign included airborne and ground-based radar and lidar observations as well as in-situ aircraft measurement of the drop-size distributions (DSD) (see ESA (1999) for details).

During CLARE'98 campaign the particle size spectra in clouds were measured from the UK MRF's C-130 aircraft with a Forward Scattering Spectrometer (FSS) and a Two-Dimensional Cloud (2DC) probes in the size ranges between 1 μm and 23.5 μm radius and between 6.25 μm and 406.25 μm radius, respectively. The available data have a 5-sec interval of averaging.

The DYCOMS-II campaign. The DYCOMS-II field campaign took place in July 2001 in Pacific Ocean near California (Stevens et al. (2002)). It was directed to collect data to study nocturnal marine stratocumulus. The main measuring part of campaign was made during 10 research flights of the NCAR's RAF EC-130Q. On this aircraft cloud droplet spectrums were measured using a set of probes: the PMS - PCASP 100; the PMS-FSSP-100; the PMS-

* *Corresponding author address*: Dr. Oleg Krasnov, IRCTR, TU Delft, Mekelweg 4, 2628 CD Delft, The Netherlands; e-mail: o.krasnov@irctr.tudelft.nl

FSSP-300; the PMS-260X; the PMS-2DC; and the PMS-2DP in the different size ranges between 0.045 and 786 μm radius. For in-situ measurements of LWC on aircraft two King hot-wire probes that were installed on different wings and the Gerber's Particulate Volume Monitor PVM-100A were used. The available data have a 1-sec interval of averaging.

The CAMEX-3 campaign. The third field campaign in the Convection And Moisture Experiment series (CAMEX - 3) took place in Florida coastal zone in August - September 1998. The objective of the field program was data collection for research in tropical cyclone using NASA-funded aircrafts ER-2 and DC-8, and ground-based remote sensing. For this study it was important that all research flights took place in cumulus clouds. For measurement of the cloud drop size distributions were used the FSS (the size range between 0.42 μm and 23.67 μm radius) and 2DC (the size range between 17.75 and 762.50 μm radius) probes that were mounted on the DC-8. The available data have a 60-sec interval of averaging.

2.2. In-situ clouds particle spectrum data processing and analysis

The description of field campaigns and their instrumentation shows that in order to obtain a complete cloud drop size distribution, the particular distributions measured by a few particle probes have to be merged. There are a few possible techniques for the merging (e.g. Baedi et al. (1999)). For this study all available probes were analyzed on an equal basis. The center size for every bin of every probe was calculated, counted concentration was normalized by the bin's width. Then all bins for the probes were combined altogether and rearranged in increasing order of their center size values. The resulting grid of center sizes was used for estimation of the values for new bounds of bins - as half distance between the centers of neighbor bins. Such approach gives the possibility to include in the analysis all available data without any a priori assumptions about the shape of DSD. The statistical moments of any order for the resulting DSD can be calculated as numerical integrals of tabulated functions. For every probe the first and last bins were not taken into consideration as possible sources of error information.

Since this study only deals with liquid water clouds, it was assumed that for radar observations the spherical drops act as Rayleigh scatterers, while for lidar observations they approximately act as optical scatterers. In that case, various cloud parameters can be computed from the particle size spectra using the equations for the spectral moments of 2nd, 3rd, and 6th order.

2.3. Cloud droplets and drizzle

In cloud physics the total DSD in water clouds usually is divided with size in two parts - small cloud droplets and big drizzle particles. The reason for such division is the difference in their formation processes, behavior, and influence on measurable variables. The threshold size for division of DSD into droplets and drizzle fractions is not fixed and well established - most of researchers are using the diameter value around 50 μm. From other point of view the answer for this question is possible to find from the available in-situ probes datasets for different measurements campaigns.

First, it is necessary to check the existence of the statistical difference between the droplets and drizzle particles. For such study we used data that were measured during the DYCOMS-II campaign with three in-situ probes: the PMS-FSSP-100 (size range 1 - 47 μm diameter); the PMS-FSSP-300 (size range 0.3 - 20 μm diameter); the PMS-260X (size range 15 - 645 μm diameter). The FSSP-100 and 260X probes were mounted on NCAR's RAF EC-130Q aircraft very close one to other, and FSSP-300 was mounted under other wing, about 35 m away. For these probes the measured concentrations have been analyzed. In despite of different size ranges and big spatial separation between two FSS probes the correlation between counted concentrations is more then 0.9 for all available DYCOMS-II data. And vice versa, the correlation between concentrations from FSSP-100 and PMS-260X, which were placed onboard at a short distance, is less then 0.1.

Such statistical independence of the cloud droplets and drizzle particles has as result two important conclusions:

- for analytical representation of the total DSD in water clouds it is necessary to use the mixture of independent DSDs, there is no way to combine characteristics of both fractions in the framework of any united distribution, and
- the statistical independence of the droplets and drizzle gives the possibility to separate and analyze the influence of every fraction on measurable variables.

Let consider now the total DSD in water clouds. Every particular spectrum does not give the information how to divide it in droplet and drizzle fractions. Such information exists only in the set of all or selected with some criterion spectra. It is possible to estimate the threshold size for separation of independent fractions of cloud particles using correlation function:

$$C(R_{thres}) = \frac{\left\langle F(0,R_{thres}) \cdot F(R_{thres},\infty) \right\rangle}{\left\langle F(0,R_{thres})^2 \right\rangle^{1/2} \cdot \left\langle F(R_{thres},\infty)^2 \right\rangle^{1/2}}, \quad (1)$$

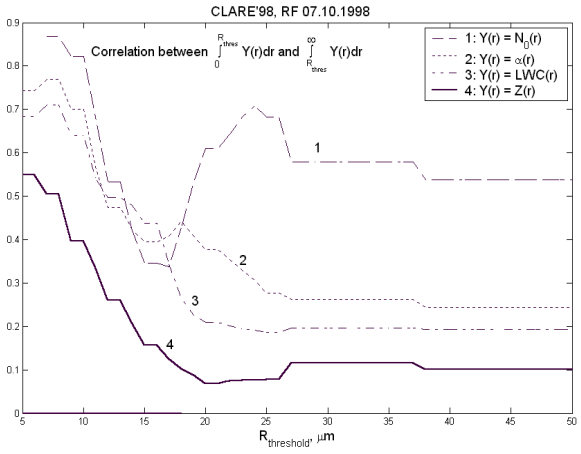

Fig. 1. The correlation between concentrations, optical extinctions, liquid water contents and radar reflectivities of cloud droplets and drizzle fractions as function of threshold size for fraction separation.

where $F(A,B) = \int_A^B Y(r)N(R)dr$, $N(r)$ is the total DSD, and $Y(r)$ is any function of drop radius r. For the correlation between the concentrations in fractions $Y(r)$ = 1, but it also possible to estimate the correlation between the optical extinctions, the liquid water contents, and the radar reflectivities of fractions. If the analyzed merged DSD can be represented as sum of two statistically independent distributions, which have quite visible difference in mean values, the correlation function (1) has to have additional minimum. The ordinate of such minimum will correspond to the statistically optimal boundary between two independent fractions. Figure 1 represents the correlation (1) between concentrations, optical extinctions, liquid water contents and radar reflectivities of cloud droplets and drizzle fractions as function of threshold size for fraction separation. These results were derived for data from the research flight of the UK MRF's C-130 aircraft on October 7, 1998 during CLARE'98 campaign near Chilbolton, UK (ESA (1999)). The additional minimum is presented on all plots. Most clear it is visible for concentration - around 17 μm radius. For radar reflectivity such minimum is wider and coincides with radius value 20-25 μm that is most often-used in drizzle studies.

Thus, in this section the possibility to use in-situ data for statistically based definition of droplets and drizzle fractions in water cloud was demonstrated. The resulting threshold radius has values between 17 and 20 μm. This is a bit less than the radius value 25 μm, which is usually used in drizzle studies (Gerber (1996)).

2.4. The estimation of drizzle fraction

The importance of possibilities to detect the presence of the drizzle fraction in clouds and to characterize it follows from the strong influence of drizzle particles on the radar measurements. The fact that radar reflectivity is proportional to the sixth moment of DSD leads to the result that small number of drizzle particles can produce the major part of the cloud's reflectivity without strong contribution in the LWC. The illustration of this fact is presented on Fig. 2, where the ratio of drizzle reflectivity to droplets reflectivity versus the ratio of drizzle LWC to droplets LWC plotted. It was calculated from merged spectra for CLARE'98 campaign data using threshold size 20 μm from previous section. From this graph follows that for most of the spectra the contribution of the drizzle fraction into total LWC becomes compatible with cloud droplets only when drizzle reflectivity exceeds the droplets reflectivity in 30-40 dB.

Because the radar reflectivity is very sensitive to the presence of big drops, the ratio of drizzle to droplets reflectivities can be selected to characterize the presence of drizzle fraction and to estimate its amount. Which remote sensing measurable quantity can be used for the estimation of such ratio? On Fig. 3 the dependence of reflectivities ratio versus total radar reflectivity is presented and it can be seen that this dependence is very widely scattered - for given value of total reflectivity the variation in drizzle to droplets reflectivities ratio can exceed 20 dB. From this representation follows that radar reflectivity alone can not characterize the presence and amount of drizzle.

From the simultaneous and collocated radar and lidar measurements it is possible to estimate another parameter - the ratio of radar reflectivity to optical extinction Z/a. The dependence of the drizzle to droplets reflectivities ratio versus this parameter for CLARE'98 data is presented on Fig. 4. This plot shows very strong correlation between analyzed parameters. For all datasets, which were used in this study, the estimated correlation coefficient is not less then 0.95. The

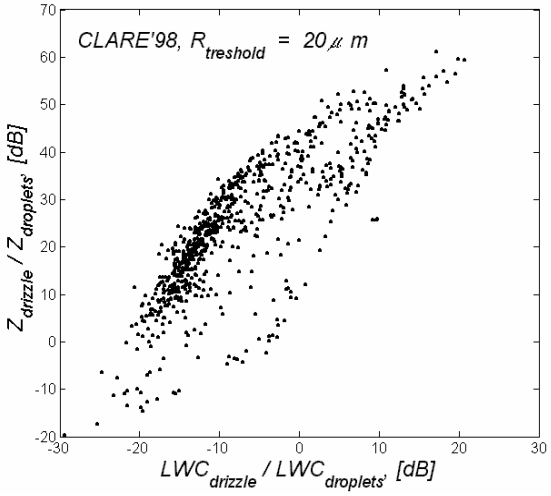

Fig. 2. The dependence between the ratio of drizzle to droplets reflectivities versus the ratio of drizzle to droplets LWCs for CLARE'98 campaign data.

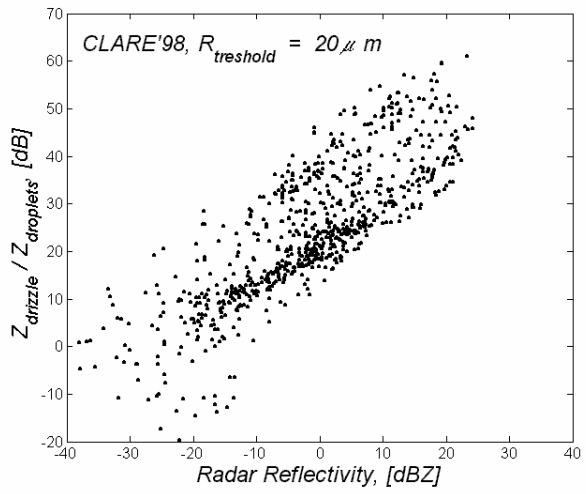

Fig. 3. The dependence of the ratio of drizzle to droplets reflectivities versus total radar reflectivity for CLARE'98 campaign data.

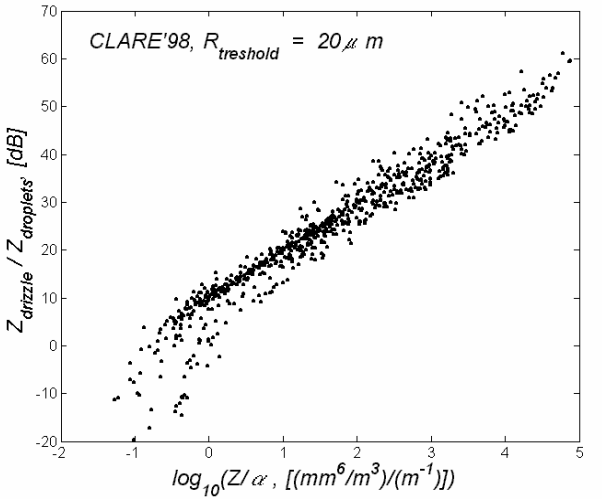

Fig. 4. The dependence of the drizzle to droplets reflectivities ratio versus the ratio of radar reflectivity to optical extinction Z/a for CLARE'98 data.

conclusion is that the Z/a ratio is very sensitive to the presence of drizzle fraction and is directly proportional with strong correlation to this fraction amount in terms of the drizzle to droplets reflectivities ratio.

For meteorological applications much more important is the estimation of drizzle influence on liquid water content in clouds. On Fig. 5 the dependence of the LWC in drizzle fraction versus the Z/a ratio for CLARE'98 data is presented. It is relatively wide scattered, but the trend of direct proportionality between these two quantities is visible, especially from the behavior of mean value. Following Gerber (1996), such representation can be used for the classification cloud with drizzle fraction into two classes - cloud with light drizzle and cloud with heavy drizzle. Because the presented dependence shows the linear relationship between drizzle LWC and radar to lidar ratio, it is not clear, which threshold value of the Z/a ratio is necessary to use for such classification. Is it possible to find such threshold value that is based on sound arguments? The answer for this question comes from the study of the relation between the Z/a ratio and the effective radius in water cloud.

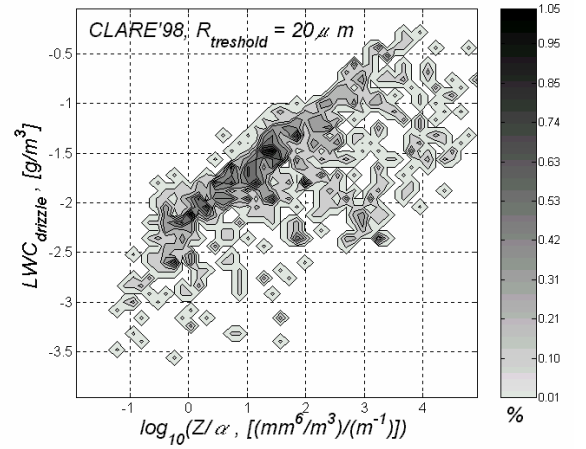

Fig. 4. The dependence of the LWC in drizzle fraction versus the Z/a ratio for CLARE'98 data.

2.5. The radar to lidar ratio versus effective radius

The merged drop size distribution data for all campaigns were depicted on the plane "ratio of radar reflectivity to optical extinction versus the effective radius" ($Z/a - r_{eff}$) (Fig. 6). On the same plot the relationships for three parameters gamma drop size distributions with two extreme values of the shape parameter n ($n = \infty$, that corresponds to the narrow, d-function-like gamma distribution, and $n = 1$, that corresponds to the exponential distribution) are presented. The conclusions that follow from this representation are:

- All data that were measured in the different geographical regions, inside the different types of water clouds, and during the different field campaigns with the different sets of the cloud's particle probes have the similar behavior. It means that the observed dependence has a stable character.
- The observed data show a complicated difference with theoretical relationships for three parameters analytical distributions. Only the part of observed DSD that are characterized by lowest value of the Z/a ratio can be described in terms of the simple statistical distributions.

Detail study (Krasnov and Russchenberg (2002)) shows that the observed $Z/a - r_{eff}$ relationship can be explained and described using a model of the mixture of independent statistical distributions, for example, modified gamma distribution for cloud droplets and exponential distribution for drizzle particles.

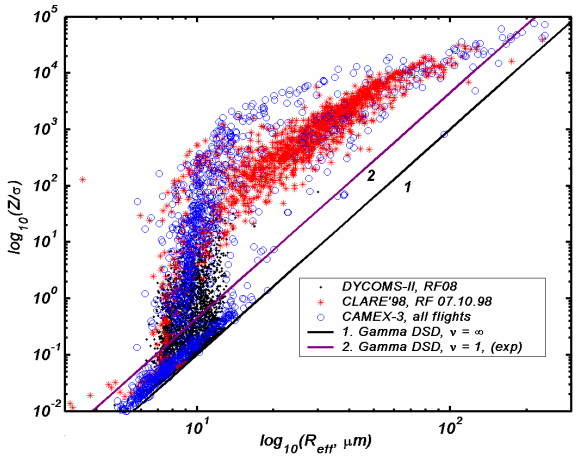

Fig. 6. The Radar to Lidar Ratio versus the Effective Radius for the CLARE'98, DYCOMS-II, and CAMEX - 3 campaigns data

The reliable fitting equation for the $r_{eff} = F\left(Z/a\right)$ dependency was found as a 4th order polynomial:

$$\lg(r_{eff}) = -0.0027(\lg(Z/a))^4 + 0.026(\lg(Z/a))^3 - \\ -0.0094\cdot(\lg(Z/a))^2 + 0.0098\cdot(\lg(Z/a)) + 0.99 \quad (2)$$

From the analysis of the observed data for all campaigns together and for every campaign separately follows that equation (2) has good agreement with the CLARE'98 and the DYCOMS-II data for stratiform clouds. For cumulus clouds, which were observed during the CAMEX-3 campaign, the noticeable difference in the region of maximal variability of the Z/a ratio can be seen - the observed effective radii in that region for a given Z/a ratio are shifted to lowest values. It can be explained as natural difference between stratiform and cumulus clouds – in cumulus clouds the drizzle fraction has to be taken into account for drop size distributions that have smallest effective radii.

The analysis of the observed $Z/a - r_{eff}$ relationship shows that its behavior changes remarkably in two points - around $\log_{10}(Z/a)$ =- 1, where influence of drizzle fraction becomes visible, and around $\log_{10}(Z/a)$ = 1.8, where very fast growing Z/a as function of the effective radius changes into slow. The last point can be used as threshold value for classification of the drizzle fraction into light and heavy classes. On Fig. 5 we can see that the value $\log_{10}(Z/a)$ = 1.8 corresponds with value 0.03 g/m^3 of mean drizzle LWC that is close to the proposed by Gerber (1996) value 0.01 g/m^3.

As result, from our analysis follows the possibility to use the Z/a ratio for classification the clouds into three types:

- "The cloud without drizzle": $\log_{10}(Z/a)$ < -1, $Z_{drizle}/Z_{droplets}$ < 0 dB, the contribution drizzle fraction into LWC is negligible, for the DSD description it is possible to use standard three parameters distributions like modified gamma or log-normal;
- "The cloud with light drizzle": -1 < $\log_{10}(Z/a)$ < 1.8, $Z_{drizle}/Z_{droplets}$ < 30 dB, the contribution of the drizzle fraction into LWC is less then 0.03 g/m^3. This class can be characterized with very fast growing of the Z/a ratio as the effective radius increases;
- "The cloud with heavy drizzle": $\log_{10}(Z/a)$ > 1.8, $Z_{drizle}/Z_{droplets}$ > 30 dB, the contribution of the drizzle fraction into LWC is essential, slow growing of the Z/a ratio as function of the effective radius, for the description of the DSD it is necessary to use the model of the mixture of independent DSD.

2.6. Application of the features of the radar to lidar ratio for the retrieval of the LWC in water clouds

Consider now the application of described above cloud type classification technique for the parameterization of the $Z-LWC$ relation in water clouds. On Fig.7 in-situ data for three campaigns on the $Z-LWC$ plane are presented. On the same plot a few known approximations for this relationship are also presented:

(a) Baedi et al. (2000):

$$Z = 57.54\cdot LWC^{5.17} \quad (3)$$

(b) Fox and Illingworth (1997):

$$Z = 0.012\cdot LWC^{1.16} \quad (4)$$

(c) Sauvageot and Omar (1987):

$$Z = 0.03\cdot LWC^{1.31} \quad (5)$$

(d) Atlas (1954):

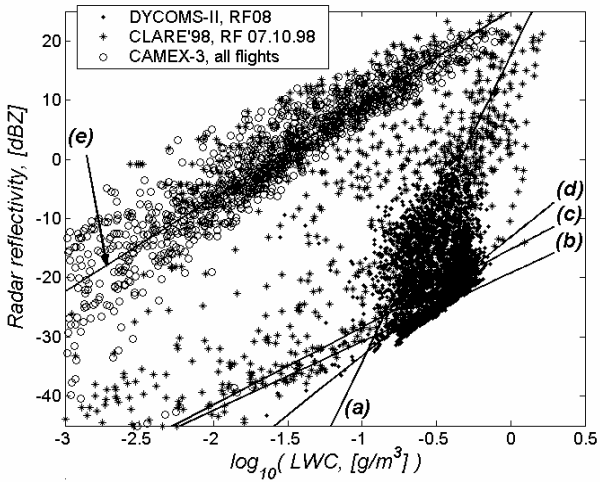

Fig.7. The relation between Liquid Water Content and Radar Reflectivity for different field campaigns. Lines represent the different linear fittings of this relation.

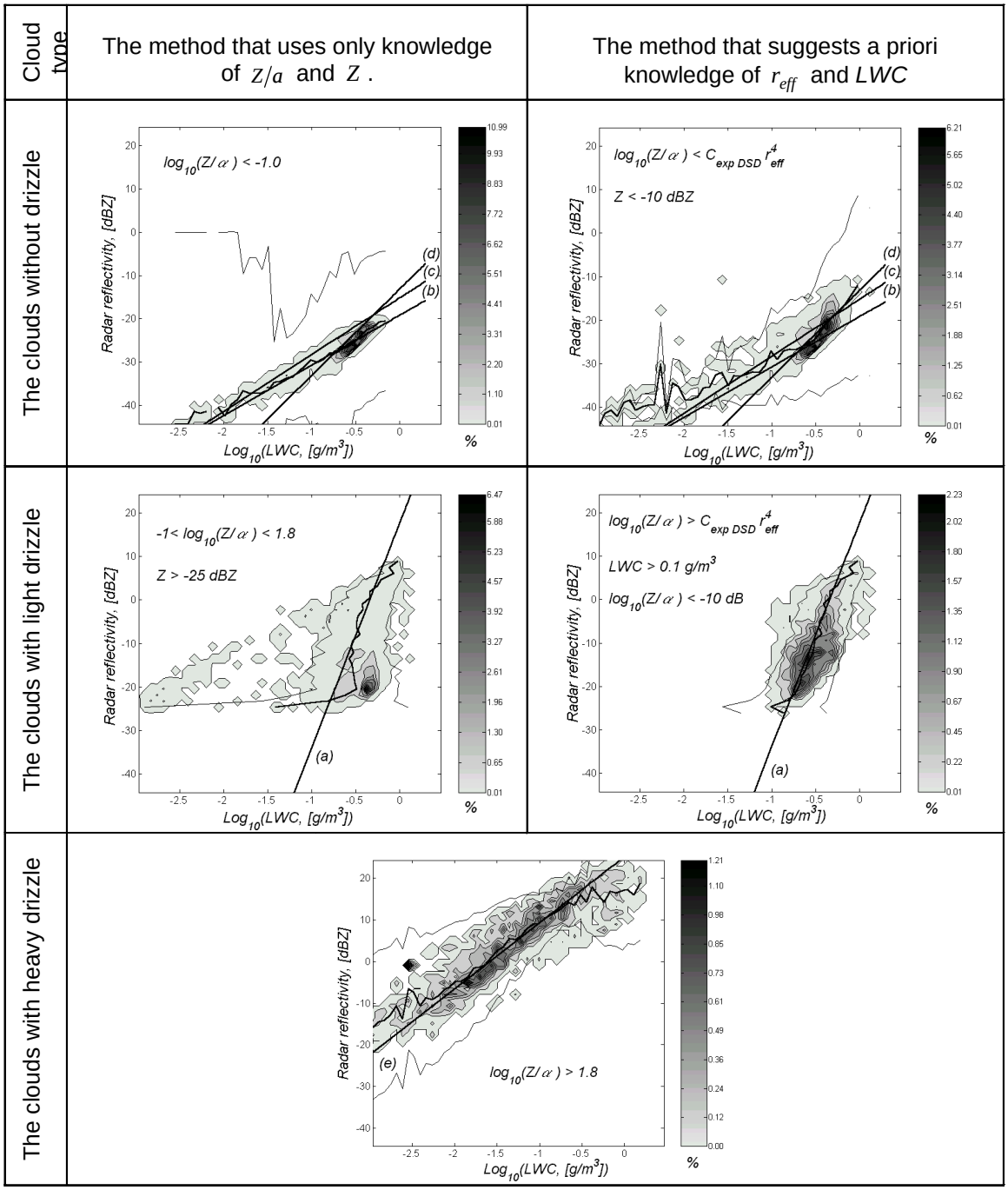

Fig. 8. Two-dimensional histograms for the relation (with mean, standard deviations, and linear fittings) for different criteria and methods of cloud's type classification

$$Z = 0.048 \cdot LWC^{2.0} \quad (6)$$

(e) Best fit of all data for the CAMEX-3 campaign and the CLARE'98's data for the drizzle clouds:

$$Z = 323.59 \cdot LWC^{1.58} \quad (7)$$

It is clear from this representation that the $Z - LWC$ relation is very scattered and not one of known analytical relationships can be used alone. From other point of view, the positions of presented data on the $Z - LWC$ plane show some tendency to concentrate around every lines (a) - (e). It gives the background for the search of the algorithm for the classification of cloud DSD into a few classes, which can be parameterized with the different $Z - LWC$ relationships. On Fig. 8 two-dimensional distributions of in-situ observed DSDs on the separate for every class $Z - LWC$ plane and related analytical relationships (a) - (e) are presented. For such classification we used two methods. Both of them use the clouds type classification with the value of Z/a ratio technique that was described in previous section. The differences are only in same additional criteria, which for the first method require the knowledge about in-situ measured parameters - r_{eff} and *LWC* and for the second

method - only the results of radar and lidar measurements of Z/a and Z. The used criteria for classification of the cloud type and selection of the $Z-LWC$ relationship also are presented on the Fig. 8. As result from Fig. 8 it can be seen that equations (b), (c), and (d) can parameterize the $Z-LWC$ relationship in the clouds without drizzle, equation (a) can be applied for the clouds with light drizzle, and (d) - for the clouds with heavy drizzle. The second important conclusion, which follows from the comparison of images in columns on Fig. 7, is that the method based only on remote sensing measurables gives practically the same classification result as the use of the complete DSD information.

3. THE SYNERGETIC RADAR-LIDAR TECHNIQUE

Following Krasnov and Russchenberg (2002), for the retrieval algorithm we have used the value of the radar reflectivity to lidar extinction ratio for the classification of the every cloud range cell on vertical profile into three classes:

"the cloud without drizzle fraction"

$$\log_{10}(Z/a) < -1,$$

"the cloud with light drizzle"

$$-1 < \log_{10}(Z/a) < 1.8,$$

"the cloud with heavy drizzle"

$$\log_{10}(Z/a) > 1.8,$$

where Z is in $[mm^6/m^3]$, and a - in $[1/m]$. These classes reflect the statistical features of the drop size distribution in given range cell and their names, proposed for cloud in-situ data interpretation, have to be used carefully for profile regions below cloud base.

For every resulting class the different Z-LWC relationship were applied:

- For the (A) class "the cloud without drizzle fraction" can be used relations (4),(5), or (6).
- For the (B) class "the cloud with light drizzle" - relationship (3).
- For the (C) class "the cloud with heavy drizzle" - relationship (7)

Large values of the optical extinction in water clouds cause situations when ground-base lidar backscattering profile (and derived optical extinction) does not cover the whole region where cloud radar reflectivity is presented. As result for such upper regions in the cloud the radar reflectivity to optical extinction ratio is unknown and described above classification algorithm could not be used. For such cloud cells a simplified classification algorithm that uses only information about the radar reflectivity is proposed. It requires two threshold values of radar reflectivity. The lower value -30 *dBZ* can be used for the classification of the "cloud without drizzle fraction" class. This value was estimated from the CLARE'98 in-situ measured cloud particles size spectra and has good agreement with others campaigns data for stratiform clouds. The second threshold value for differentiation the clouds with "light" and "heavy" drizzle fractions using the similar procedure was selected to be equal to -20 *dBZ*. This value has much less stable character for in-situ datasets and during application of the algorithm to the real remote sensing data it can be used like tuning parameter with control of the retrieval results.

The resulting retrieval procedure can be summarized as follows. From the simultaneous and spatially matched radar and lidar data the classification map for cloud cells using Z/a (where this parameter was available) and/or Z values was produced. For every of three resulting cloud cells classes - "the cloud without drizzle fraction", "the cloud with light drizzle", and "the cloud with heavy drizzle", the different Z-LWC relationships have to be used. The application of such relationships to the radar reflectivity profiles produces the *LWC* profiles. These profiles integration over the height produce the retrieved *LWP*, which can be compared with *LWP* from the microwave radiometer for new technique results validation.

4. THE APPLICATION TO CLOUDNET DATA

CloudNET is a research project supported by the European Commission under the Fifth Framework Programme. The project has been done in April 2001 – September 2005, aimed to use data obtained quasi-continuously for the development and implementation of cloud remote sensing synergy algorithms. The use of active instruments (lidar and radar) resulted in multi-year continuous time series of detailed vertical profiles of important cloud parameters. A network of three cloud remote sensing stations: Chilbolton - UK, Cabauw - the Netherlands, and Palaiseau – France, were operated continuously starting September 2001 until now, data formats harmonized and joint, analysis of the data performed to evaluate the representation of clouds in four major european weather forecast models (UK Met Office meso-scale operational model, ECMWF operational model, Meteo France operational model, and KNMI (the Netherlands) RACMO operational model). Remote sensing synergy techniques for the ice and water cloud parameters retrievals were developed in the framework of the project and applied to measured data to produce different level products. The detail description of the Cloudnet project, available measured data and products descriptions and access gateway can be found on Internet site www.met.rdg.ac.uk/ radar/cloudnet/index.html.

4.1. Observational data used

For the purpose of this study the radar-lidar synergy technique was applied to simultaneous, spatially-collocated, calibrated, and synchronized data from the cloud radars and lidars at every Cloudnet site to produce the retrieved liquid water contents of low level clouds. The results validation has been done using the comparison with the liquid water path (LWP) that was independently retrieved from microwave radiometer data. The remote sensing sites that participated in the Cloudnet project had quite similar instrumentation and represent the measured data in the same time scale (averaging time 30 seconds) and formats (conventional netCDF files).

Remote sensing instrumentation at Cabauw, the Netherlands (51.971° North, 4.927° East) includes Vaisala CT75K lidar ceilometer (wavelength 905nm, range resolution 30 m, integration time 15 seconds, working range up to 11.25 km), 35-GHz cloud radar (working frequency 34.86 GHz, beam width 0.36 degrees, range resolution 90 m, working range 0.2 - 13 km), and 22 channel microwave radiometer MICCY - MIcrowave Radiometer for Cloud CarthographY (Crewell et al. (1999)) . The continuously measured radar/lidar data with range resolution 90 m available for 1068 days during the period August 2001 - March 2005. Unfortunately, the available measurements with microwave radiometer covers far less days.

Remote sensing instrumentation at Chilbolton, UK (51.1445° North, 1.4370° West) includes Vaisala CT75K lidar ceilometer (wavelength 905nm, range resolution 30 m, integration time 15 seconds, working range up to 11.25 km), 94-GHz cloud radar Galileo (working frequency 94.00 GHz, beam width 0.5 degrees, range resolution 60 m, working range up to 12 km), and dual frequency microwave radiometer (working frequencies 22.2/28.8 GHz). The continuous radar/lidar data with range resolution 60 m in addition to microwave radiometer data available for 447 days during the period April 2003 - September 2004.

Remote sensing instrumentation at Palaiseau site near Paris, France (48.713° North, 2.204° East) includes LD40 ceilometer (wavelength 855 nm, resolution up to 8 m, integration time 15 seconds, working range up to 13 km), 95-GHz cloud radar RASTA (working frequency 95.04 GHz, beam width 0.2 degrees, range resolution 60 m, working range up to 15 km) and microwave radiometer Drakkar (working frequencies 23.8/36.5 GHz, Beam width 13.3/11.0 degrees, integration time: 0.25 – 2.0 seconds). The continuous radar and lidar data with range resolution 60 m in addition to microwave radiometer data available for 289 days during the period January 2003 - September 2004. The peculiarity of this site's data is that during most of available days the simultaneous measurements did not cover whole 24 hours, they were done preferably during daytime.

The radars cross-calibration between all three sites has been done during special campaign when RASTA radar from Palaiseau traveled to Chilbolton and Cabauw. The resulting corrections for radar reflectivities were taken into account for production of calibrated data. There is also possibility to make cross-comparison of the lidars. The ceilometers in Chilbolton and Cabauw are the same type and, as result – quite similar characteristics. The LD40 ceilometer in Palaiseau is owned by KNMI and before the Cloudnet project long time worked at Cabauw simultaneously with CT75K lidar ceilometer. These data are available for analysis and cross-comparison.

4.2. Cloudnet target categorization product

Together with calibrated data for particular instruments in the Cloudnet database the product "Instrument Synergy/Target Categorization" has been included, which is intended to facilitate the application of multi-sensor algorithms by performing much of the required preprocessing. It includes radar, lidar, microwave radiometer, rain gauge and model data with regridding, correction for attenuation, reporting of measurement errors, data quality flags and categorization of targets. The detailed description can be found in Hogan and O'Connor (2004). For the presented study this product had been used as input for the LWC retrieval algorithm. The reason is that for the application of radar-lidar retrieval technique synchronized in time and range radar and lidar data are necessary. In addition, the developed technique is applicable only for radar/lidar scattering on water drops and needs an additional filter, which will remove from consideration all reflections that are influenced by ice and any other non-water drops reflections. Such categorization is done using all the data available and the description of algorithms can be found in Hogan and O'Connor (2004).

To apply the radar-lidar technique for LWC retrieval the "atmospheric water" mask was used. Such mask includes only pixels where small liquid droplets or falling hydrometeors are with temperature above 0° C are present and gives an assurance that LWC retrievals will be done only for applicable regions. From other point of view such mask produces the LWC map, which is bounded from above by zero isotherm. For cases with the presence of supercooled water it will result in underestimation of integral LWP and produce additional discrepancy between proposed technique and microwave radiometer's LWP.

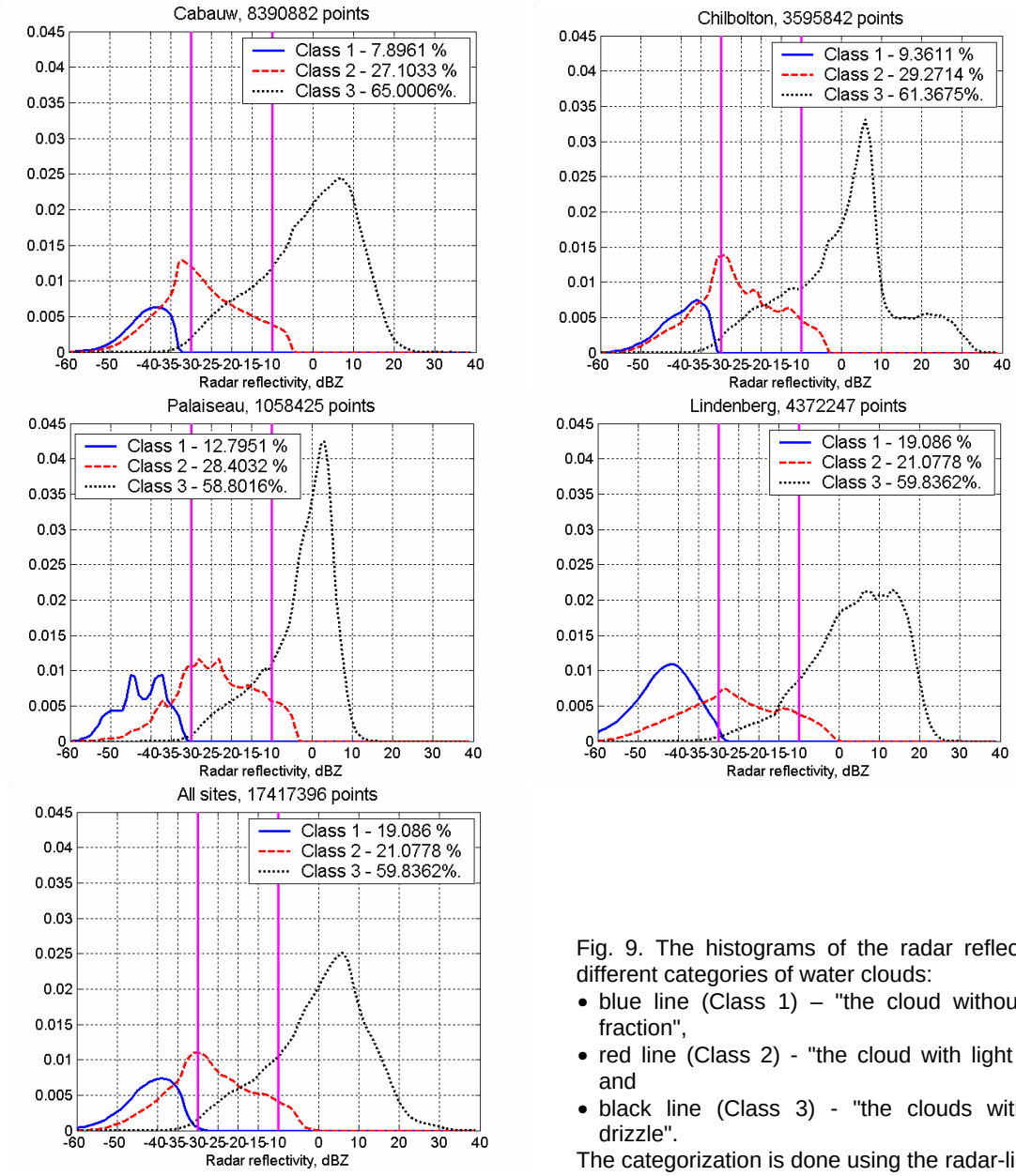

Fig. 9. The histograms of the radar reflectivity for different categories of water clouds:

- blue line (Class 1) – "the cloud without drizzle fraction",
- red line (Class 2) - "the cloud with light drizzle", and
- black line (Class 3) - "the clouds with heavy drizzle".

The categorization is done using the radar-lidar ratio

4.3. Estimation of the lidar extinction profiles

In this study for the lidar extinction profiles estimation we have used Klett (1981) inversion algorithm that involves only one boundary value for the solution of the lidar equation: the absolute extinction on some reference level, which have to be as far from the lidar as possible. This method requires assume the power-law relationship between range dependent lidar backscattering coefficient $b(h)$ and optical extinction $a(h)$ in the form $b(h) = k_1 \cdot a(h)^{k_2}$. For water clouds that are optically thick the k_2 coefficient is considered to be unity in almost all studies (Rocadenbosch and Comeron (1999), Rogers *et al*. (1997)). For the reduction of the noise influence on stability of the inversion algorithm in this study we have used clipping procedure for zeroing nearest to lidar range cells and all range cells in profile that are less then some threshold value. This threshold noise level has been calculated for every profile. After such clipping for each profile the farthest non-zero range bin was used as reference level.

4.4. Algorithm improvement

One of the critical points in the proposed radar-lidar synergy technique is the reliable threshold values of the radar reflectivity for the cases when the liquid water categorization has to done using only radar information. As it was noted in section 3, from the analysis of in-situ droplet distribution have been derived the values -30 dBZ and -20 dBZ. The huge amount collected during the Cloudnet data, which represent practically all possible meteorological situations, gives nice possibility to check and statistically improve the these constants.

Such analysis can be done using data from cloud regions, where the radar to lidar ratio

Z/a is known. Using this parameter for liquid water categorization it is possible to count the histograms of radar reflectivity for every water cloud category - "the cloud without drizzle fraction", "the cloud with light drizzle", and "the clouds with heavy drizzle", and use them for estimation statistically reliable threshold values of reflectivity. Such histograms for every particular site and for whole Cloudnet database are presented on Fig. 9.

A few conclusions follow from this representation, giving some additional proves in correctness of the basic principles of proposed

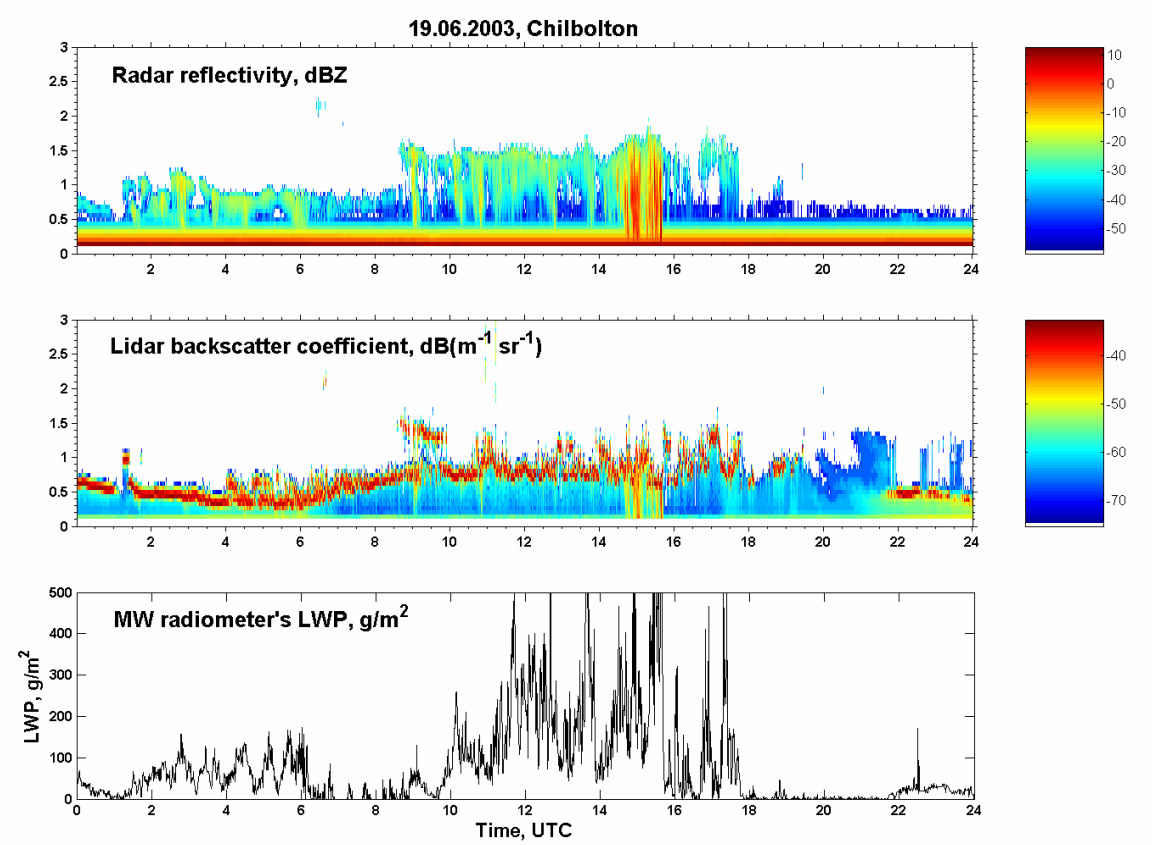

Fig. 10. The temporally and spatially matched radar, lidar and radiometer measurements for one observational day during the Cloudnet project, June 19, 2003, at Chilbolton.

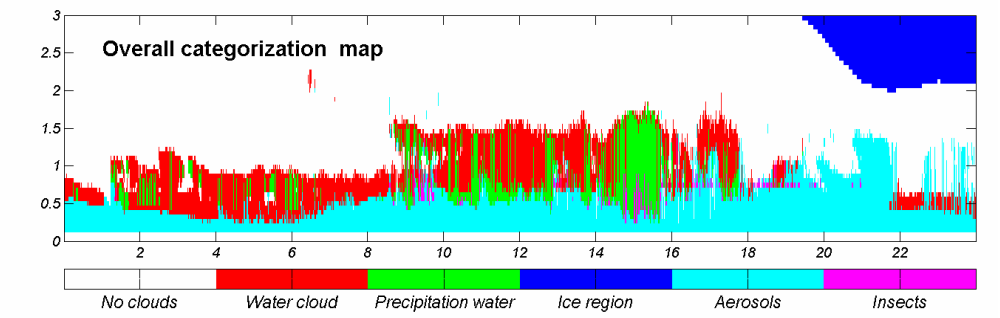

Fig. 11. The Cloudnet target categorization map, June 19, 2003, at Chilbolton

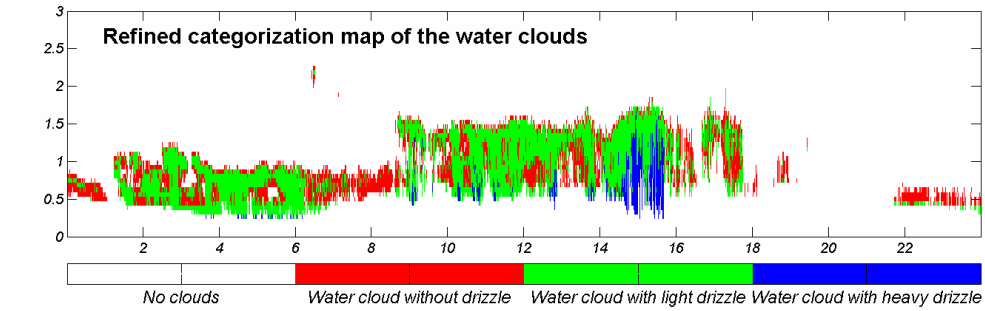

Fig. 12. This liquid water categorization for June 19, 2003, at Chilbolton, derived from radar-lidar ratio.

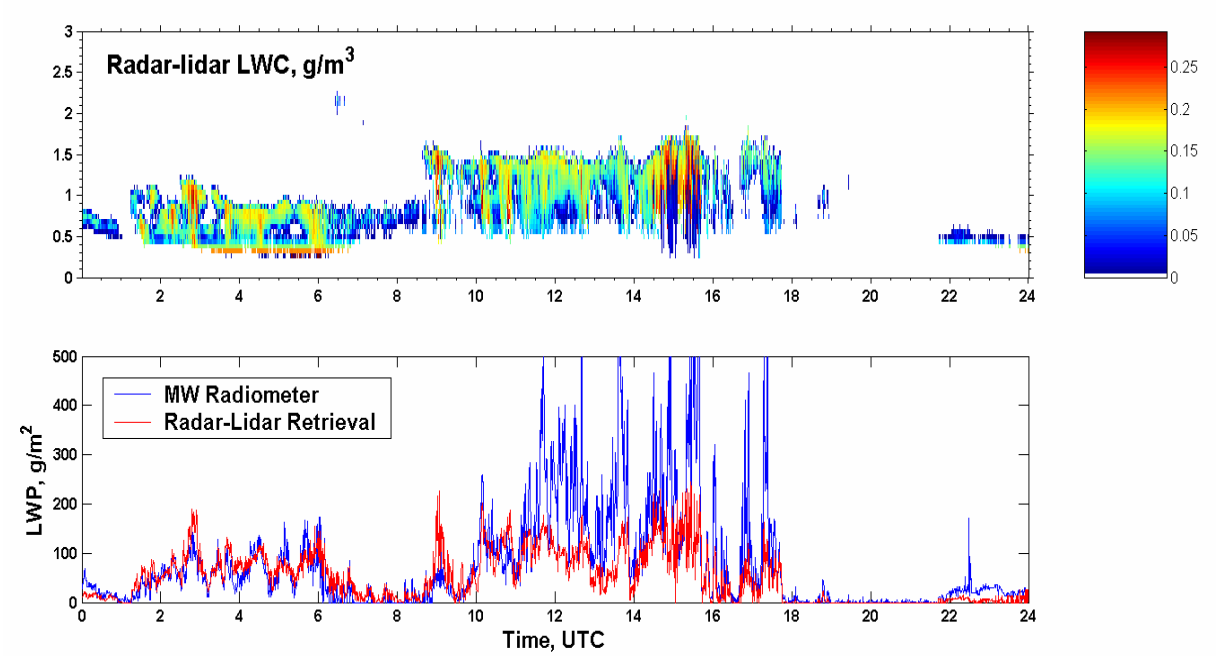

Fig. 13. The map of LWC, retrieved from radar reflectivity using the synergetic radar-lidar technique (upper plot), and the integral LWP, in comparison with LWP, measured by microwave radiometer (lower plot).

technique.

First, all three Cloudnet sites look in terms of presented histograms quite similar. The percentages of cases when specific cloud types are observed are very closed: 8.7% - "the cloud without drizzle fraction", 27.8% - "the cloud with light drizzle", and 63.5% - "the clouds with heavy drizzle". For all three sites there are no observations of "the cloud without drizzle fraction" with radar reflectivity greater -30 dBZ – complete agreement with in-situ data. From other point of view, in many cases "the cloud with light drizzle" has radar reflectivity around -30 dBZ. It looks reasonable for the minimization errors in incorrect water clouds categorization to use the point of histogram intersection – in this case it gives the threshold value -35 dBZ instead -30 dBZ. The second threshold value -20 dBZ, which is in use for the discrimination between "the cloud with light drizzle" and "the clouds with heavy drizzle", looks very reasonable and reliable.

4.5. Retrieval results and discussion

The described above technique to the whole available Cloudnet database was applied and the processing results were included in this database as new level 2 product. It is organized as daily netCDF files and includes 30 seconds averaged optical extinction profiles, derived from lidar signals, the ratio of radar reflectivity to optical extinction profiles, the LWC profiles, the bit field of water cloud categorization as "the cloud without drizzle fraction", "the cloud with light drizzle", and "the clouds with heavy drizzle", the time series of integrated LWP and the time series of optical depth, derived from lidar's optical extinction. Currently processed data include 1124 days for Cabauw, 447 days for Chilbolton, 289 days for Palaiseau, and 550 days for Lindenberg. These data and quicklooks are available on-line on the Cloudnet web-site.

As example, on Fig. 10 presented temporally and spatially matched radar, lidar and radiometer measurements for one observational day, June 19, 2003, at Chilbolton. This day is quite interesting as combination of different water cloud types and precipitation. In time interval 1.00 - 6.00 UTC the thin drizzling stratiform clouds with cloud top around 1000 m above see level can be seen, then clouds become non-precipitating, and between 9.00 – 18.00 thick drizzling and rain clouds with cloud top up to 1500 m above see level are presented. For whole day the cloud top is well below zero isotherm and ice and melting process can be excluded from drizzle and rain formation in this case.

On Fig. 11 the Cloudnet categorization map is shown and makes clear meteorological situation and the nature of observations for this day. This map was used to filter only signals, reflected by atmospheric liquid water objects, and to apply for such reflections described in chapter 3 categorization based on radar to lidar ratio for regions with known optical extinction or based only on the radar signals for the regions where lidar signal was completely attenuated. The resulting liquid water categorization map presented on Fig. 12. In spite of the fact that for this map production only proposed technique was used, it show quite natural and physically understandable drizzle distribution within the clouds.

This liquid water categorization map was used for the selection of Z-LWC relationship,

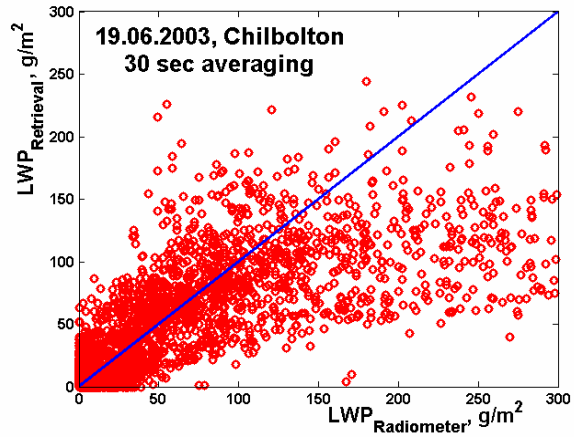

Fig. 14. The scattering diagram of the radar-lidar retrievals versus radiometer data, for the cases when microwave radiometer's liquid water path was less then 400 g/m^2

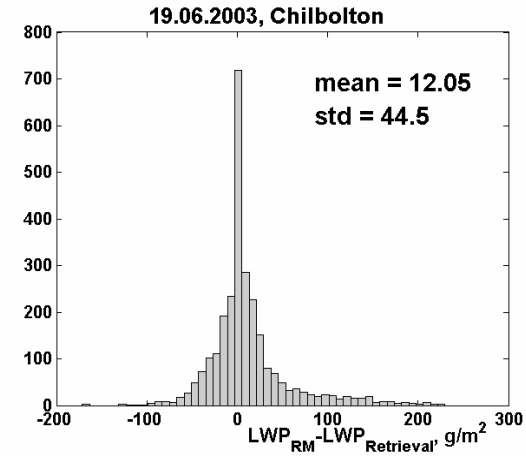

Fig. 15. The histogram of the difference in microwave radiometer's and radar-lidar LWPs, for the cases when microwave radiometer's liquid water path was less then 400 g/m^2

applicable for given category of cloud cell, and, as result, for the conversion of radar reflectivity into LWC profiles. The results of such retrieval are presented on upper plot of Fig. 13. The integration of resulting LWC over vertical profile gives liquid water path, which can be compared with independent measurements from microwave radiometer. Such comparison as time series represented on lower plot on Fig. 13.

The analysis of this plot shows very good correlation and reasonable agreement for situations when both algorithms are applicable without any doubt – for this day it takes place until 9.00 UTC. For the interval 9.00 – 18.00 UTC with heavy precipitation the agreement is not so good, although the correlation still visible. But it is known fact that the question "How trustable is microwave radiometer measurements of LWP during precipitation?" is still open. To prevent this topic discussion, which is well outside of the framework of presented study, all cases when microwave radiometer's liquid water path was larger then 400 g/m^2 were excluded from consideration. The scattering diagram of the radar-lidar retrievals versus radiometer data is presented in Fig. 14 and shows good agreement in retrievals up to 150 g/m^2 and non-linear relation above. The resulting histogram of the difference in microwave radiometer's and radar-lidar LWPs presented on the Fig. 15. It demonstrate quite reasonable statistical bias 12 g/m^2 and standard deviation 44.5 g/m^2, which has practically the same order as random error of microwave radiometer's LWP itself).

5. THE COMPARISON OF THE LIQUID WATER PATH (LWP) DERIVED FROM OBSERVATIONS AND NUMERICAL WEATHER MODELS

The long-term near-continuous observations and numerical models output for the four ground-based stations in Europe (Chilbolton, Cabauw, Palaiseau, and Lindenberg), which were collected during the Cloudnet project, provide good opportunity for the retrieval algorithms and models verification and validation, through the selected variables of interest inter-comparison. This chapter is devoted to the statistical analysis and inter-comparison of the liquid water path (LWP) multiyear dataset, retrieved from observations and provided by a few different numerical weather modes.

5.1. Numerical models data

For this study the available numerical weather models data, which were collected during the Cloudnet project, were analyzed. Such collection includes the ECMWF model (horizontal resolution 40 km), the KNMI regional atmospheric climate model (RACMO) (horizontal resolution 18 km), the Met Office mesoscale model (Horizontal resolution 12 km), the Met Office global model (horizontal resolution 60 km), the Meteo France Model (horizontal resolution 23.4 km), the Swedish Meteorological and Hydrological Institute the Rossby Centre Regional Atmosphere (SMHI RCA) model (horizontal resolutions 44 and 24 km), and the Deutscher Wetterdienst Lokal (DWD LM) model (horizontal resolution 7 km). All model data are presented as 1 hour averaged time series for the cell of the model grid collocated with every ground-based station. As the liquid water content represented in model data as the gridbox-mean liquid water mixing ratio Q_l, it was necessary to convert it into liquid water mass per volume unit:

$$LWC = \frac{P \cdot Q_l}{287.05 \cdot T} \ [\text{g/m}^2],$$

where P and T are the pressure and temperature variables, also available as model output.

5.2. Observational data and retrievals

In the framework of the Cloudnet project a few techniques were used to retrieve the information about liquid water clouds contents from observations.

All ground-based stations were equipped with multichannel microwave radiometers, which measure the sky brightness temperatures on different frequencies in zenith direction. These temperatures then were converted to the LWP using site-specific retrieval techniques.

Two techniques to provide the vertical profiles of the LWC were developed and used during the Cloudnet project – the scaled adiabatic method and the radar-lidar technique. As soon the scaled adiabatic retrieval technique uses microwave radiometer LWP for the integral constrain the LWC profiles, it does not produce any useful information for LWP comparison and was not considered in this study.

5.3. Data processing

As the observations and retrieval results are presented in the Cloudnet database with 30 sec averaging time, before the comparison with numerical model data, which have 1 hour sampling interval, it was necessary to regrid microwave radiometer and radar-lidar LWP into models time grid. It was done through the averaging of observations during 1 hour interval before the model time.

It is known fact that microwave radiometer LWP with values greater then 400 g/m^2 are affected by precipitations and in most cases are untrustable. In this study two types of statistical analysis were used - using whole available LWP dataset and using datasets after filtration out all values of LWP, which are greater than 400 g/m^2. The first approach was used to estimate common behavior of the analyzed data, and the second one was used for intercomparison of different LWP data sources to prevent possible influence of errors, coming from differences in sensitivity of the retrievals to precipitations, in sampling policy during precipitation at different ground stations, etc.

As soon as the radar-lidar LWC profiles are bounded from above with zero isotherm, the numerical models LWP are calculated with the same height limitations to minimize the bias in intercomparison. For the comparison with microwave radiometer retrievals the whole height profile of the models LWC is using for the LWP calculation.

5.4. The results and discussion

The mean and standard deviation values of the LWP for all available in the Cloudnet models and retrievals presented in Figure 16. These figures represent the values, which were calculated after filtration out the LWP data with values greater than 1000 g/m^2 for every source.

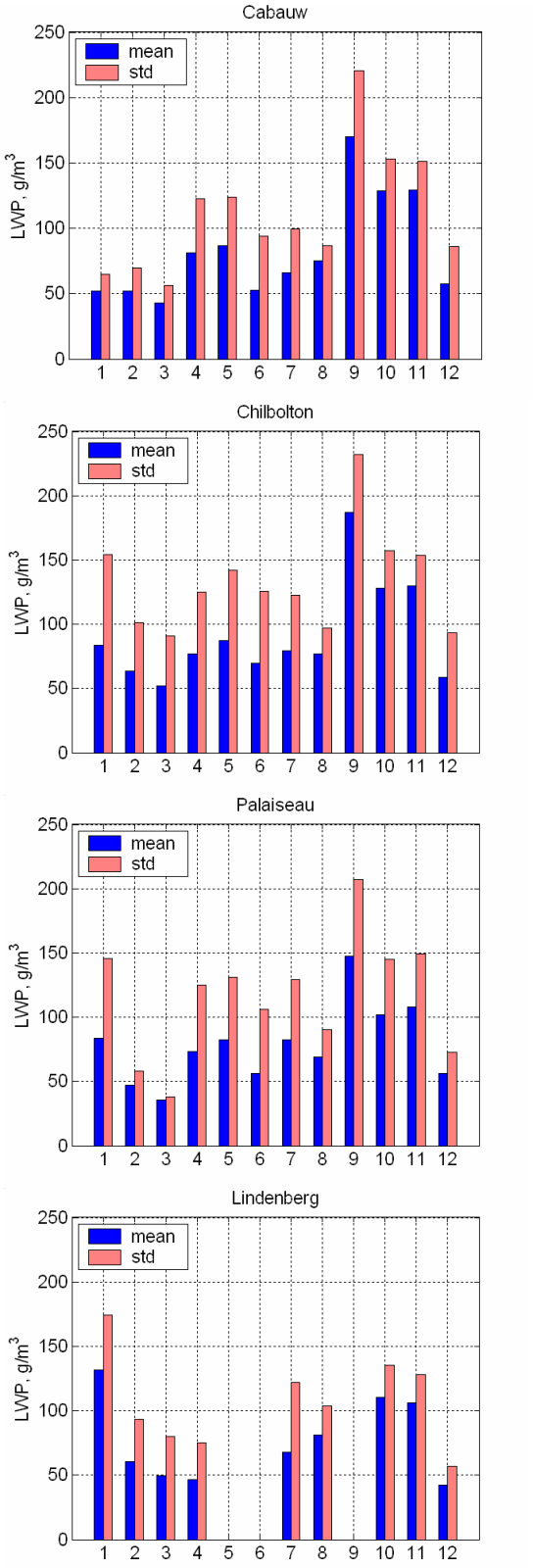

Fig 16. The values of the mean and standard deviation for the LWP from Cloudnet observations and numerical models. The abscissa notation: **1** - MW Radiometer; **2** - Radar/Lidar technique, in-situ thresholds; **3** - Radar/Lidar technique, Cloudnet; thresholds; **4** - ECMWF model; **5** - RACMO model; **6** - Met Office Mesoscale 6-11 model; **7** - Met Office Global model; **8** - Meteo France model; **9** - SMHI RCA model; **10** - SMHI RCA L24 model; **11** - SMHI RCA L40 model; **12** - DWD LM-6-17 model

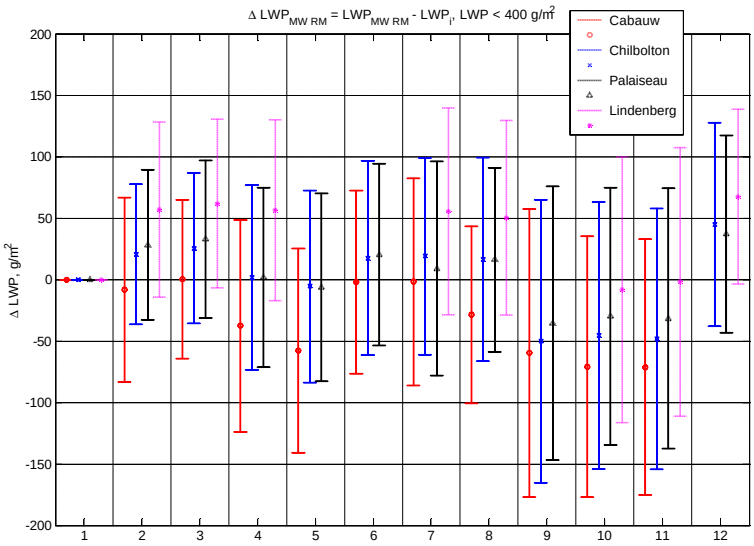

(a)

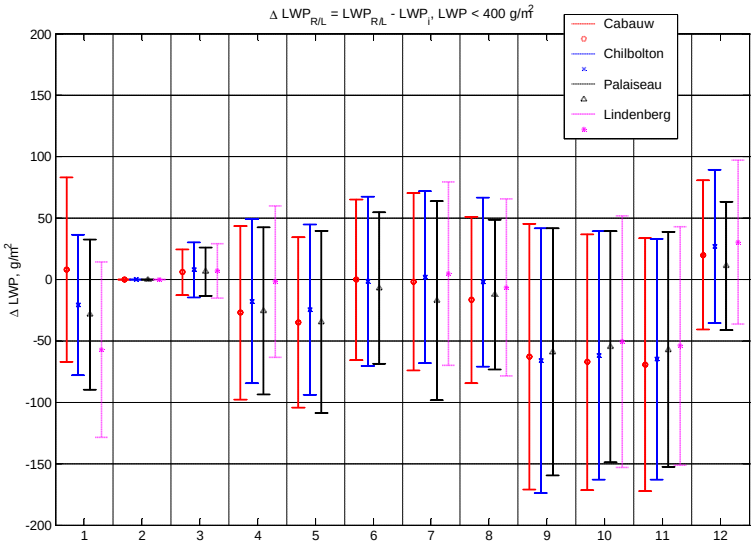

(b)

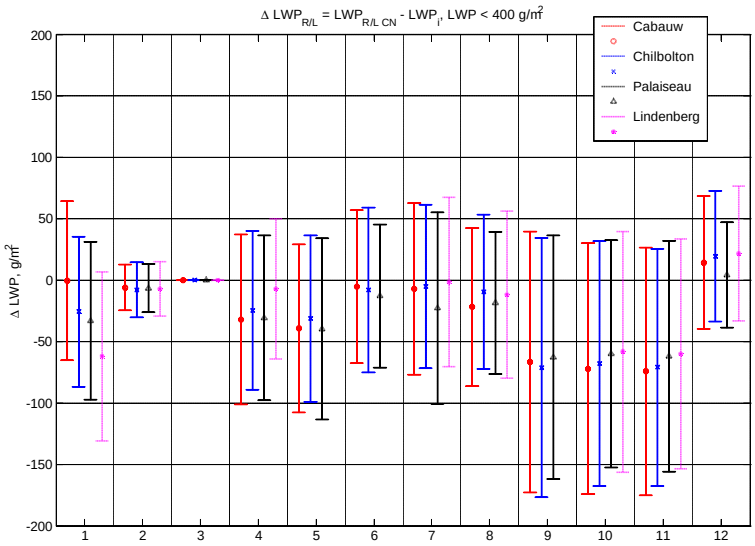

(c)

Fig. 17. The differences between retrieved form observations LWP (a) microwave radiometer, b) radar/lidar technique, c) radar/lidar technique with Cloudnet radar reflectivity thresholds, and other retrievals and models output. The notation of the abscissa is the same as in Fig. 16.

In Figure 17 represented the statistics of differences between three retrieved from observations LWP and other retrieved and models LWPs – Fig 17(a) plots differences $LWP_{MWRM} - LWP_i$ for microwave radiometer, Fig. 17(b) – for the radar-lidar technique with original thresholds values for radar only water clouds categorization, and Fig. 17(c) – for radar-

lidar technique with thresholds values for radar only water clouds categorization that derived from the whole set of the Cloudnet radar/lidar data. The statistics for such differences derived using data subsets, which are forming only by cases when both selected variables are available.

From this representations follow a few quite interesting conclusions.

The standard deviation of all analyzed LWP dataset are bigger then their mean values. It means that the probability distributions fall faster around zero value and have longer tails then exponential distribution. The filtration out samples with outlaying values does not help much.

All numerical models can be categorized into three groups accordingly to the mean value of LWP. First group, which produced minimum LWP, includes the Met Office mesoscale and global models, the Meteo France, and DWD LM. The ECMWF and RACMO models, which produce about two times bigger LWP, form the second group. And third group includes the SMHI RCA model, which produce more LWP than the models of first group.

The radar/lidar technique produce quite similar statistics over all Cloudnet ground stations, which is quite close to the statistical parameters of the first group of numerical models (the Met Office mesoscale and global models and the Meteo France)

The behavior of the microwave radiometer LWP looks quite different for different sites. For the Cabauw site the results are not affected strongly by the filtration out the big values. The reason is that the provided LWP data were already filtered with the maximum value 500 g/m^2.The Chilbolton and Palaiseau data look quite similar and strongly affected with outlaying values – after filtration the variability coefficient (std/mean) drops into 2 times from 3 to 1.5-1.6. The comparison of the radiometers data with models also produce site-dependent results – from Fig. 16 follows that for Cabauw site good agreement with measurements have the models of the first group (the Met Office mesoscale and global models and the Meteo France), and for Chilbolton and Palaiseau sites – the models of the second group (the ECMWF and RACMO models).

The reasons of such variability in microwave radiometers data can be found in the differences of the retrieval techniques, which are in use on different sites. At the Cabauw site the simple interpolation technique was used to convert MICCY microwave radiometer brightness temperatures into LWP. At the Chilbolton and Palaiseau more improved approach has been used. An additional source of difference can be in the different policy of radiometer work during the rain events. At Cabauw the MICCY radiometer simply switches off during the precipitation and it can explain the absence of huge values of LWP with 1 hour averaging.

The radar/lidar technique, which was applied to every Cloudnet site in the same way and, as follows from Fig.17, show quite stable and similar results for all sites, helps to detect such variability in radiometers LWP. To use this technique, which provide completely independent from microwave radiometer and reliable information about water clouds even in cases of the drizzle presence, is quite important for the numerical models verification and improvement.

6. CONCLUSIONS

Using set of in-situ data that were measured during different field campaigns in different geographical regions inside different types of water clouds was shown:

- Very good characteristics for the detection and parameterization of the drizzle fraction in water clouds has the ratio between radar reflectivity and optical extinction;
- The presence of stable $Z/a - r_{eff}$ relationship for the different geographical locations, different field campaigns and different cloud types. It is possible to use for all analyzed campaigns and cloud types a unified 4th order polynomial fitting of this relationship;
- The possibility to classify water clouds into three types – “the cloud without drizzle”, “the cloud with light drizzle”, and “the cloud with heavy drizzle”, using the ratio Z/a of radar reflectivity to optical extinction;
- The possibility to retrieve LWC from radar reflectivity using different types of the $Z-LWC$ relationships for the cloud without drizzle, for the cloud with light drizzle, and for the cloud with heavy drizzle. For the classification of the cloud cell into such three types is possible to use only parameters that are available for measurements with radar and lidar.

These results used as background for the development of new enhanced algorithm for the retrieval of liquid water cloud properties from simultaneous radar and lidar measurements. This method uses the value of the ratio of radar reflectivity to lidar optical extinction for the classification of cloud's range cells into three types - "the cloud without drizzle fraction", "the cloud with light drizzle", and "the clouds with heavy drizzle". The subsequent application for every resulting type of the cloud's cells the specific Z - LWC relationship allows to retrieve LWC in low level clouds.

The proposed technique for the *LWC* retrieval has been applied for the dataset, collected in the framework of the Cloudnet project on four European remote sensing sites: Chilbolton - UK, Cabauw - the Netherlands,

Palaiseau – France, and Lindenberg - Germany. Totally it includes 2410 days of observation.

The comparison of the radar-lidar technique retrievals with integrated liquid water contents from microwave radiometer shows good correlation and reasonable agreement for situations when both algorithms are applicable. For the cases without precipitation, when microwave radiometer's liquid water path is less then 400 g/m^2, the statistical difference between radiometer's and proposed technique's integral water content is of the order of 50 g/m^2.

REFERENCES

Atlas, D., 1954: The estimation of cloud content by radar. *J. Meteor*., **11**, 309-317.

Baedi, R. J. P., J. J. M. de Wit, H. W. J. Russchenberg, J. P. V. Poiares Baptista, 1999: Alternative algorithm for correcting FSSP measurements, *Proc. Int. workshop CLARE'98*, ESA-ESTEC, 123-127.

Crewell, S, G. Haase, U. Löhnert, H. Mebold, C. Simmer, 1999: A ground based multi-sensor system for the remote sensing of clouds. *Phys. Chem. Earth (B*), **24**, 207 - 211

ESA, 1999: CLARE'98: *Cloud Lidar And Radar Experiment, International Workshop Proceedings. WPP* - 170, ISSN 1022-6556, ESTEC, Noordwijk, The Netherlands, 239 pp.

Fox, N. I. and A. J. Illingworth, 1997: The retrieval of stratocumulus cloud properties by ground-based cloud radar. *J. Appl. Meteor*., **36**, 485-492.

Hogan, R. J. and O'Connor, E. J., 2004: Facilitating cloud radar and lidar algorithms: the Cloudnet Instrument Synergy/Target Categorization product. / *Cloudnet project documentation.* – available on-line: http://www.met.rdg.ac.uk/~swrhgnrj/publications/categorization.pdf

Gerber, H., 1996: Microphysics of Marine Stratocumulus Clouds with Two Drizzle Modes, *J. Atmos. Sci.*, 53 (12), 1649-1662.

Klett, J. D., 1981: Stable analytical inversion solution for processing lidar returns. *Appl. Opt*., **17**, 211 - 220.

Krasnov, O. A., and H. W. J. Russchenberg, 2002: The Relation Between the Radar to Lidar Ratio and the Effective Radius of Droplets in Water Clouds: An Analysis of Statistical Models and Observed Drop Size Distributions. In *Proc. 11th AMS Conf. on Cloud Physics, Orden, Utah, USA, 3-7.06.2002*.

Rocadenbosch, F., and A. Comeron, 1999: Error Analysis for the Lidar Backward Inversion Algorithm. *Appl. Opt*, **38**, 4461 - 4474

Rogers, R. R., M. - F. Lamoureux, L. R. Bissonnette, R. M. Peters, 1997: Quantitative Interpretation of Laser Ceilometer Intensity Profiles. *J. Atmos. Oceanic Technol.*, **14**, 396 - 411

Sauvegeot, H. and J. Omar, 1987: Radar reflectivity of cumulus clouds. *J. Atmos. Oceanic Technol.*, **4**, 264-272.

Stevens, B., D. H. Lenschow, G. Vali, et al, 2002: Dynamics and Chemistry of Marine Stratocumulus – DYCOMS-II. *Bulletin of the American Meteorological Society*, **84**(5), pp. 579-593.